Formation of a Phosphorus−Phosphorus Bond by Successive One-Electron Reductions of a Two-Phosphinines-Containing Macrocycle: Crystal Structures, EPR, and DFT Investigations

Laurent Cataldo,[†] Sylvie Choua,[†] Théo Berclaz,[†] Michel Geoffroy,*[,†] Nicolas Mézailles,[‡] Louis Ricard,[‡] François Mathey,*[,‡] and Pascal Le Floch*[,‡]

Contribution from the Department of Physical Chemistry, 30 Quai Ernest Ansermet, University of Geneva, 1211 Geneva, Switzerland, and Laboratoire "Hétéroéléments et Coordination", UMR CNRS 7653, Ecole Polytechnique, 91128 Palaiseau Cedex, France

Received February 6, 2001. Revised Manuscript Received April 3, 2001

Abstract: Chemical and electrochemical reductions of the macrocycle **1** lead to the formation of a radical monoanion anion $[\mathbf{1}]^{\bullet-}$ whose structure has been studied by EPR in liquid and frozen solutions. In accord with experimental ^{31}P hyperfine tensors, DFT calculations indicate that, in this species, the unpaired electron is mainly localized in a bonding σ P−P orbital. Clearly, a one-electron bond (2.763 Å) was formed between two phosphorus atoms which, in the neutral molecule, were 3.256 Å apart (crystal structure). A subsequent reduction of this radical anion gives rise to the dianion $[\mathbf{1}]^{2-}$ which could be crystallized by using, in the presence of cryptand, Na naphthalenide as a reductant agent. As shown by the crystal structure, in $[\mathbf{1}]^{2-}$, the two phosphinine moieties adopt a phosphacyclohexadienyl structure and are linked by a P−P bond whose length (2.305(2) Å) is only slightly longer than a usual P−P bond. When the phosphinine moieties are not incorporated in a macrocycle, no formation of any one-electron P−P bond is observed: thus, one-electron reduction of **3** with Na naphthalenide leads to the EPR spectrum of the ion pair $[\mathbf{3}]^{\bullet-}$ Na^+; however, at high concentration, these ion pairs dimerize, and, as shown by the crystal structure of $[(\mathbf{3})_2]^{2-}[\{Na(THF)_2\}_2]^{2+}$ a P−P bond is formed (2.286(2) Å) between two phosphinine rings which adopt a boat-type conformation, the whole edifice being stabilized by two carbon−sodium−phosphorus bridges.

I. Introduction

Recent reports on the chemistry of phosphorus have pointed out the unique electronic properties of this element which allow for the preparation of new structural moieties which cannot be obtained with carbon or nitrogen analogues.[1−3] Most of these structural properties of organophosphorus compounds are related to the reluctance of this element to form hybrids from s and p orbitals and to adopt trigonal planar bonding geometries. This suggests that, for reagents containing multiple phosphorus−carbon bonds,[4] the phosphorus coordination in the reaction product can be affected by factors which modify the molecular flexibility. Such systems could be potentially interesting in the context of chemical sensors since, for example, the opening or closing of a chemical bond could be provoked by the addition or removal of an electron.[5] In the present paper, we explore this possibility by studying the one-electron reduction product of a system involving two phosphinine moieties **a** (Chart 1).

Chart 1

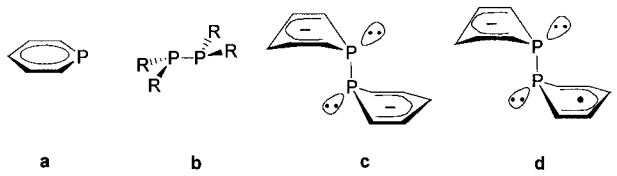

By analogy with the dimerization of the phosphinyl radical $R_2P^{\bullet}$ which gives rise to the compound of structure **b**,[6] dimerization of the phosphinine radical anion is likely to lead to the dimeric structure **c**. Reaction between a phosphinine anion and a neutral phosphinine (**d**) to give a compound corresponding to the one-electron oxidation product of **c** is much less realistic since the dimerization is disfavored by loss of the aromaticity of the phosphinine ring. P−P bond formation may, however, be envisaged by forcing the two phosphorus atoms to be close to each other and to have their π^* orbitals oriented along the same direction; a one-electron reduction of this system could then place the extra electron in a molecular orbital having a bonding character between the two phosphorus atoms. We will show that this strategy can be successfully followed by incorporating two phosphinine rings in a macrocycle which maintains them in the desired stereochemistry (Chart 2).

[†] University of Geneva.
[‡] Ecole Polytechnique.

(1) Grützmacher, H. *Science* **2000**, *289*, 737−738.
(2) Kato, T.; Gornitzka, H.; Baceiredo, A.; Schoeller, W. W.; Bertrand, G. *Science* **2000**, *289*, 754−756.
(3) Canac, Y.; Bourissou, D.; Baceiredo, A.; Gornitzka, H.; Schoeller, W. W.; Bertrand, G. *Science* **1998**, *279*, 2080.
(4) Regitz, M.; Scherrer, O. J. *Multiple Bonds and Low Coordination in Phosphorus Chemistry*; Georg Thieme: New York, 1990. Dillon, K. B.; Mathey, F.; Nixon, J. F. *Phosphorus: The Carbon Copy*; John Wiley: New York, 1998.
(5) Kaifer, A. E.; Gomez-Kaifer, M. *Supramolecular Electrochemistry*; Wiley-VCH: New York, 1999.
(6) (a) Fritzsche, H.; Hasselrodt, U.; Korte, F. *Angew. Chem., Int. Ed. Engl.* **1964**, *3*, 64. (b) Spanier, E. J.; Caropreso, F. E. *Tetrahedron Lett.* **1969**, 199. (c) Low, H.; Tavs, P. *Tetrahedron Lett.* **1966**, 1357. (d) Hinchley, S. L.; Morrison, C. A.; Rankin D. W. H.; Macdonald, C. L. B.; Wiacek, R. J.; Cowley, A. H.; Lappert, M. F.; Gundersen, G.; Clyburne, J. A. C.; Power, P. P. *Chem. Commun.* **2000**, 2045.

10.1021/ja010331r CCC: $20.00
Published on Web 06/16/2001

Chart 2

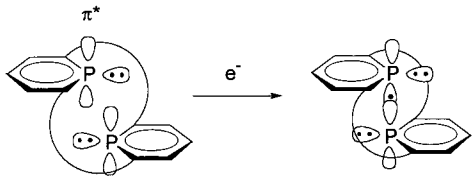

II. Results

II.1. Reduction Experiments. Reduction with Sodium Naphthalenide: Crystal Structures and EPR Spectra of the Reduction Compounds. Our experiments were carried out with macrocycle **1** whose synthesis was recently reported[7] and whose crystal structure is given in the present paper. This macrocycle, which is the smallest phosphinine-based macrocycle[8] reported to date,[7] presents the appropriate geometrical requirements to test our initial hypothesis (Chart 3).

Chart 3

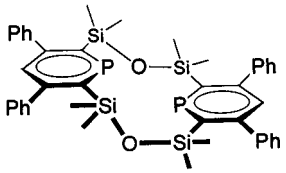

1

An ORTEP view of **1** is shown in Figure 1 as well as the most significant bond lengths and bond angles. As can be seen, the two phosphinine rings lie in two roughly parallel planes, and the distance between the phosphorus atoms is rather short (about 3.256 Å). Furthermore, we postulated that the two Si−O−Si bridges would be sufficiently flexible to allow a contact between the two phosphorus atoms upon reduction. Reduction of **1** was carried out using sodium naphthalenide at room temperature. A purple color immediately developed around the surface of the powder when the solution of sodium naphthalenide was added to **1**. After addition of 1 equiv of the reducing agent, both EPR and ^{31}P NMR spectra were recorded. The EPR spectrum (Figure 2) exhibited hyperfine coupling with two spin $^1/_2$ nuclei and was attributed to the radical monoanion $[\mathbf{1}]^{\bullet-}$, whose identification and structure are discussed in the next section. Despite the presence of this paramagnetic species, a ^{31}P NMR signal was detected; its chemical shift (δ(THF) = 2.5 ppm) was different from that of **1** (δ(THF) = 285.0 ppm) and, as shown below, reflected the formation of $[\mathbf{1}]^{2-}$.

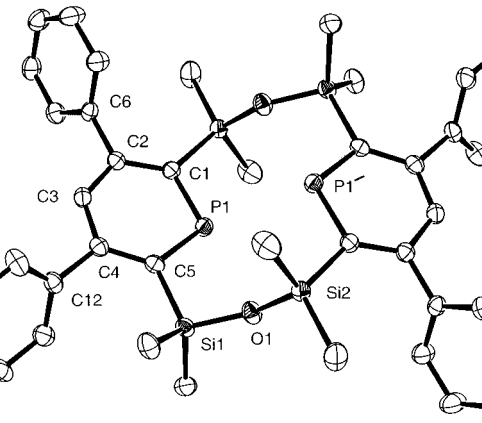

Figure 1. ORTEP drawing of one molecule of **1**. The labeling is different from that used for the NMR spectra. Selected bond lengths (Å) and angles (deg): P1−C1, 1.744(2); C1−C2 1.405(2); C2−C3, 1.400(2); C3−C4, 1.402(2); C4−C5, 1.407(2); C5−P1, 1.739(2); C2−C6, 1.493(2); C4−C12, 1.493(2); C5−Si1, 1.891(2); Si1−O1, 1.642(1); O1−Si2, 1.857(2); P1−C1−C2, 121.3(1); C1−C2−C3, 122.6(2); C2−C3−C4, 126.1(2); C4−C5−P1, 121.2(1); C5−P1−C1, 105.87(8); P1−C5−Si1, 113.0(1); C5−Si1−O1, 106.24(7); Si1−O1−Si2, 145.49(8).

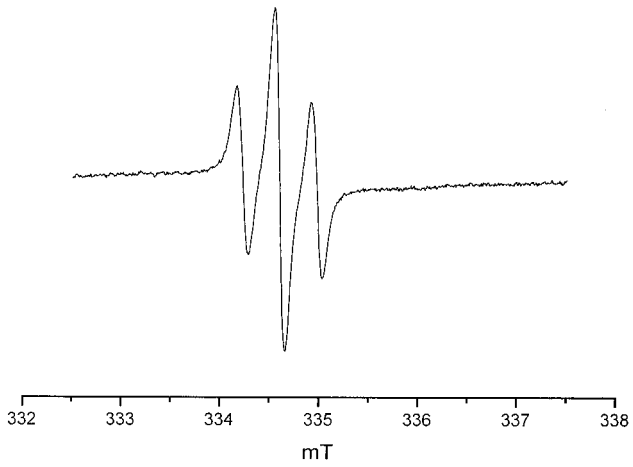

Figure 2. EPR spectrum obtained at room temperature after reduction of **1** with a solution of Na naphthalenide in THF.

We then logically focused our efforts on determining the structure of the two reduced species. Unfortunately, many attempts aimed at crystallizing the paramagnetic species $[\mathbf{1}]^{\bullet-}$ failed when crystallizations were carried out from the reaction medium. More interesting results were obtained by using cryptand (2.2.2). Surprisingly, the formulation of the crystallized species does not correspond to that of the expected mono radical anion $[\mathbf{1}]^{\bullet-}$ but to that of the minor dianionic species consisting of a $[\mathbf{1}]^{2-}$ unit and two $[Na(2.2.2)]^{+}{}_2$ units (Chart 4).

Chart 4

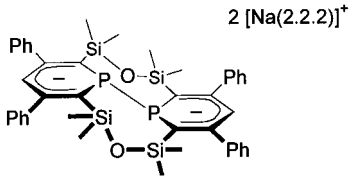

[1]²⁻[{Na(2.2.2)}₂]²⁺

The structure of $[\mathbf{1}]^{2-}[\{Na(2.2.2)\}_2]^{2+}$ was ascertained by an X-ray crystal structure. An ORTEP view of this molecule is presented in Figure 3 with the most relevant bond distances and bond angles. As can be seen, a rather long P−P bond (2.305(2) Å) has been created between the two phosphinine rings. To accommodate this particular geometry, each phosphorus atom lies out of the plane defined by the carbocyclic system (torsion angle $C_4-C_2-C_1-P_1 = 7.9°$). A close inspection of bond distances in each ring reveals a phosphacyclohexadienyl-type structure with single P−C bonds (average 1.85 Å). As the yield in $[\mathbf{1}]^{2-}[\{Na(2.2.2)\}_2]^{2+}$ turns out to be rather important (about 35%), and in accordance with the

(7) Mézailles, N.; Maigrot, N.; Hamon, S.; Ricard, L.; Mathey, F.; Le Floch, P. *J. Org. Chem.* **2001**, *66*, 1054−1056.

(8) Avarvari, N.; Mézailles, N.; Ricard, L.; Le Floch, P.; Mathey, F. *Science* **1998**, *280*, 1587.

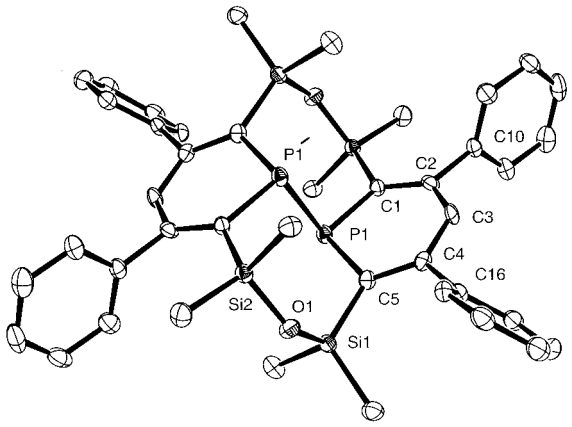

Figure 3. ORTEP drawing of one molecule of $[\mathbf{1}]^{2-}[Na(2.2.2)]^{+}_2$. The labeling is different from that used for DFT calculations and NMR spectra. The two $[Na(2.2.2)]^+$ moieties have been omitted for clarity. Selected bond lengths (Å) and angles (deg): P1−C1, 1.855(4); C1−C2, 1.384(5); C2−C3, 1.411(5); C3−C4, 1.407(5); C4−C5, 1.393(5); C5−P1, 1.845(4); P1−P1′, 2.305(2); C1′−Si2, 1.850(4); C5−Si1, 1.842(4); Si1−O1, 1.653(3); O1−Si2, 1.651(3); Si2−C8, 1.872(4); C2−C10, 1.504(5); C4−C16, 1.494(5); P1−C1−C2, 118.8(3); C1−C2−C3, 125.9(3); C2−C3−C4, 125.0(3); C3−C4−C5, 125.0(3); C4−C5−P1, 119.(3); C5−P1−C1, 102.8(2); P1−C5−Si1, 114.4(2); C5−Si1−O1, 111.8(1); Si1−O1−Si2, 137.8(2).

small equilibrium constant ($K \cong 5.95\ 10^{-5}$) deduced from the cyclic voltammetry of **1**, we propose that its formation could result not only from the crystallization of the small amount of $[\mathbf{1}]^{2-}$ present in the medium just after the reduction but also from the disproportionation of two molecules of $[\mathbf{1}]^{\bullet-}$. More conventionally, synthesis of $[\mathbf{1}]^{2-}$ species (^{31}P NMR: δ(THF) = +2.5 ppm) could be achieved by reacting 2 equivs of sodium naphthalenide with 1 equiv of **1** in THF. Formulation of this species as $[\mathbf{1}]^{2-}[\{Na(THF)_2\}_2]^{2+}$ was established on the basis of ^{1}H and ^{13}C NMR data. Indeed, ^{13}C NMR data are in good agreement with those reported by Ashe[9] on phosphacyclohexadienide anions of the parent phosphinine C_5H_5P. Whereas the chemical shifts of the carbon atoms located in ortho and para position to the phosphorus atom are strongly shielded ($\delta(C_{ortho})$ = 93.0 ppm for $[\mathbf{1}]^{2-}$ versus 195.5 ppm for **1** and $\delta(C_{para})$ = 100.6 ppm for $[\mathbf{1}]^{2-}$ versus 131.6 ppm for **1**) and that of carbon in meta position remains roughly unmodified ($\delta(C_{meta})$ = 157.7 ppm for $[\mathbf{1}]^{2-}$ versus 153.3 ppm for **1**). Addition of 2 equivs of cryptand (2.2.2) to a solution of $[\mathbf{1}]^{2-}[\{Na(THF)_2\}_2]^{2+}$ cleanly yielded $[\mathbf{1}]^{2-}[\{Na(2.2.2)\}_2]^{2+}$ (Scheme 1). Obviously $[\mathbf{1}]^{2-}[\{Na(2.2.2)\}_2]^{2+}$ is also diamagnetic and its δ^{31}P(THF) chemical shift (8.8 ppm) is reasonably close to that measured for the THF solvated species (2.5 ppm).[10]

Scheme 1

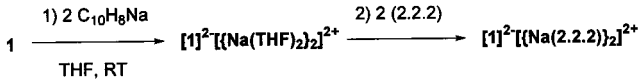

The intramolecular dimerization of $[\mathbf{1}]^{2-}$ raises the problem of the dimerization of radical anions of phosphinines. To shed light on this phenomenon, the reduction of the 3,5-dimethyl-2,6-bis(trimethylsilyl)phosphinine **3** was studied by using the same experimental conditions (THF, room temperature) as those used for the reduction of **1**. Synthesis of phosphinine **3** was carried out following a reported procedure which involves the reaction of diazaphosphinine **2** with two trimethylsilylpropyne in excess (eq 1).[11]

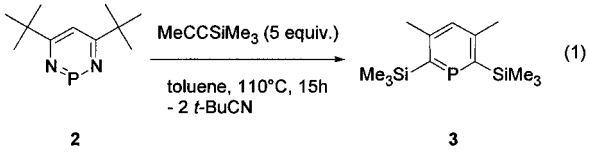

Addition of one or less equivalent of sodium naphthalenide to **3** (powder) provoked a transient red color around the powder's surface and rapidly yielded a green solution whose EPR spectrum is shown in Figure 4. The corresponding hyperfine structure results from coupling with one ^{31}P nucleus, one proton, and one ^{23}Na nucleus (natural abundance = 100%, I = 3/2). This hyperfine structure is consistent with the formation of the ion pair $[\mathbf{3}]^{\bullet-}Na^+$. As explained in the experimental part, green crystals deposited within five minutes in the reaction solution. A X-ray diffraction study showed that dimerization of the radical monoanion $[\mathbf{3}]^{\bullet-}$ indeed occurred to yield $[(\mathbf{3})_2]^{2-}[\{Na(THF)_2\}_2]^{2+}$ (Scheme 2).

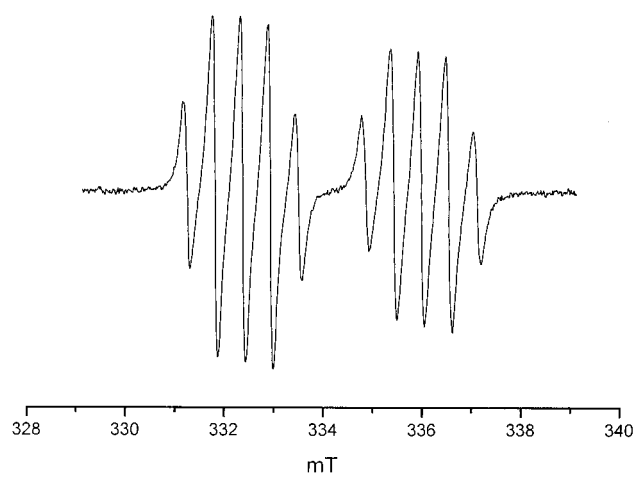

Figure 4. EPR spectrum obtained at 200 K after reduction of **3** with a solution of Na naphthalenide in THF.

An ORTEP view of the resulting species $[(\mathbf{3})_2]^{2-}[\{Na(THF)_2\}_2]^{2+}$ is presented in Figure 5 with the most significant bond lengths and bond angles. The presence of two sodium cations which are surrounded by two molecules of THF and bound to the para carbon atom (C_3 or $C_{3'}$) and to the phosphorus atom ($P_{1'}$ or P_1) of the second subunit is worth noting. This particular arrangement implies that, like in $[\mathbf{1}]^{2-}[\{Na(2.2.2)\}_2]^{2+}$, the phosphorus atom has now acquired a pyramidal geometry and both phosphinine rings adopt a boat-type conformation: the phosphorus atom P_1 and the C_3 carbon atoms deviate out of the plane defined by the four other carbon atoms ($C_4-C_2-C_1-P_1$ = 20.4°, $C_1-C_5-C_4-C_3$ = 9.6°). In both dianions, the P−P bond distances are similar (2.286(2) Å in $[(\mathbf{3})_2]^{2-}[\{Na(THF)_2\}_2]^{2+}$ and (2.305(2) Å) in $[\mathbf{1}]^{2-}[\{Na(2.2.2)\}_2]^{2+}$.

One-Electron Reduction by Electrolysis or by Reaction on an Alkali Metal Mirror: EPR Spectra. Whereas geometry of **1** and its dianion could be obtained from their crystal structures, information on the structure of the one-electron reduction product $[\mathbf{1}]^{\bullet-}$ could only be obtained from EPR

(9) (a) Ashe, A. J., III; Smith, T. W. *Tetrahedron Lett.* **1977**, 407. (b) Rosa, P.; Mathey, F.; Le Floch, P. *Chem. Commun.* **1999**, 537.

(10) Unfortunately, the poor solubility of $[\mathbf{1}]^{2-}[\{Na(2.2.2)\}_2]^{2+}$ precluded the recording of a ^{13}C NMR spectrum.

(11) (a) Avarvari, N.; Le Floch, P.; Mathey, F. *J. Am. Chem. Soc.* **1996**, *118*, 1978. (b) Avarvari, N.; Le Floch, P.; Ricard, F. *Organometallics* **1997**, *16*, 4089.

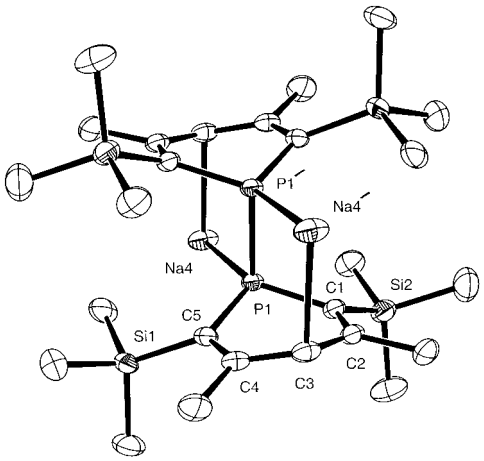

Figure 5. ORTEP drawing of one molecule of $[\mathbf{3}]_2^{2-}[Na(THF)_2]^+_2$. The labeling is different from that used for NMR spectra. The four THF co-ligands coordinated at sodium atoms have been omitted for clarity. Selected bond distances (Å) and angles (deg): P1−C1, 1.832(4); C1−C2, 1.387(5); C2−C3, 1.419(5); C3−C4, 1.413(5); C4−C5, 1.401(5); C5−P1, 1.814(4); C2−C9, 1.496(5); C4−C15, 1.502(5); C5−Si2, 1.856(4); C1−Si1, 1.869(4); C3−Na1, 2.566(4); P1−Na1′, 2.856(2); P1−P1′, 2.286(2). P1−C1−C2, 116.3(3); C1−C2−C3, 124.6(4); C2−C3−C4, 123.2(4); C3−C4−C5, 123.4(4); C4−C5−P1, 116.4(3); C5−P1−C1, 101.2(2); P1−C1−Si1, 19.6(2); P1−C5−Si2, 118.7(2); C3−Na1−P1′, 86.0(1).

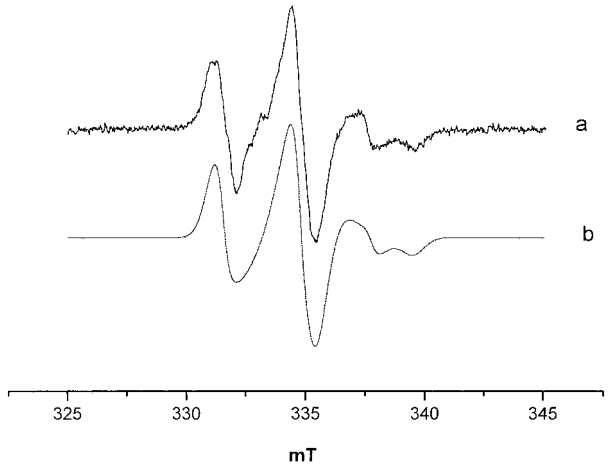

Figure 6. (a) experimental EPR spectrum obtained at 120 K with a frozen solution of $\mathbf{1}^-$ in THF. (b) Simulated spectrum.

spectra. Experimental conditions were therefore chosen to favor the specific formation of this radical monoanion: dilute homogeneous solutions, electrochemical reduction of **1** in situ in the EPR cavity at various temperatures, rapid reaction of **1** on an alkali metal mirror at low temperature under high vacuum. Similar experiments were carried out with the phosphinine **3**.

Macrocycle 1. Electrochemical reduction of a solution of **1** in THF or CH_2Cl_2, at 200 K, leads to a purple solution whose EPR spectrum is characterized by an isotropic coupling constant of 10.5 MHz with two spin $^1/_2$ nuclei. This spectrum, which is identical to the spectrum recorded after reaction of **1** with Na naphthalenide (see above, Figure 2), drastically broadens when temperature decreases. It becomes very anisotropic when the solution is frozen and, as shown in Figure 6a, spreads over ∼10 mT. The same EPR spectra were obtained by reducing, at 200 K, a solution of **1** in THF, CH_2Cl_2, or DME on a sodium or potassium mirror. By reacting with the alkali metal, the solution becomes purple.

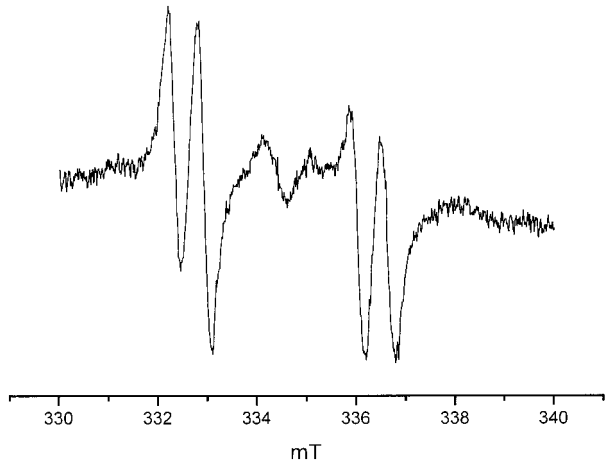

Figure 7. EPR spectrum obtained at 273 K after reaction of a THF solution of **3** on a Na mirror.

The large anisotropy of the EPR spectrum recorded at 120 K, indicates that a rather large hyperfine interaction with phosphorus nuclei occurs, but that the corresponding principal values are of opposite signs to explain the small isotropic coupling constant (10.4 MHz) observed at 200 K and attributed to two ^{31}P nuclei. This 1−2−1 triplet observed with liquid solutions results either from the coupling with two phosphorus atoms occupying magnetically equivalent positions in the molecule or from a rapid chemical exchange between two magnetically inequivalent sites. The determination of the EPR tensors was complicated by the fact that several sets of tensors lead to an acceptable simulation of the frozen solution spectrum. In a first step, the simulation was carried out by assuming two inequivalent phosphorus nuclei. The optimization led, after diagonalization, to the following set of tensors (set 1)[12] {**g**: 2.0064, 2.0041, 2.0159; $T_1(^{31}P)$: −36.8, −46.1, 109.4 MHz, $T_2(^{31}P)$: −63.3, 0.0, 135.9 MHz} which implies an averaged isotropic coupling constant equal to 16.5 MHz. Then, the simulation was performed by assuming two magnetically equivalent phosphorus nuclei at low temperature. The following set of tensors (set 2) {**g**: 2.0088, 2.0097, 2.0039; $T_1(^{31}P) = T_2(^{31}P) = -87.2, -57.3, 114.6$ MHz } was obtained after optimization; the associated isotropic coupling constant is equal to −9.7 MHz. The two sets of values correspond to ^{31}P isotropic constants whose absolute values are rather close to the value measured in liquid solution; however, the *g*-anisotropy which is obtained by assuming a dynamic process (first set) is surprisingly large for a species delocalized on carbon and phosphorus atoms (for a phosphinyl radical[13] trapped in a single crystal of $(C_6H_5)_2PS$ the **g** tensor is equal to 2.0021, 2.0039, 2.0094). The second set of values, which leads to the simulated spectrum shown in Figure 6b, seems therefore more consistent with a radical anion derived from **1**; this conclusion will be confirmed by DFT calculations (vide infra).

Phosphinine 3. Whereas no EPR spectrum could be obtained by electrolysis of **3**, a pale yellow solution of **3** in THF turns red after contact with a sodium mirror[14] at 273 K and leads to the spectrum shown in Figure 7. This spectrum exhibits a hyperfine splitting of 104 MHz with a single ^{31}P nucleus and of (−)18 MHz with a proton (probably the proton located para to the phosphorus atom) and is consistent with isotropic

(12) In this model the two ^{31}P hyperfine tensors are not aligned. These tensors, before diagonalization, are given as Supporting Information.

(13) Geoffroy, M.; Lucken, E. A. C.; Mazeline, C. *Mol. Phys.* **1974**, *28*, 839.

(14) Reaction of **3** on a potassium mirror leads immediately to a black solution without any EPR signal.

Scheme 2

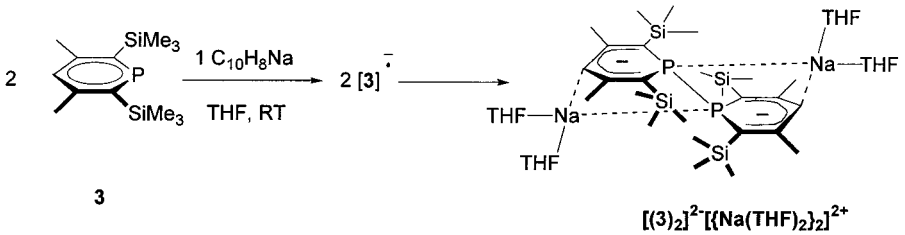

constants previously reported by Gerson et al.[15] for the 2−6-diphenylphosphinine radical anion. As mentioned above, when the reduction of **3** is carried out by adding less than 1 equiv of naphthalenide sodium to a solution of **3** in THF, the resulting solution (purple in the beginning of the addition, then green-brownish) gives rise to an EPR spectrum (Figure 4) which exhibits not only coupling with ^{31}P (100 MHz) and a proton ((−)16 MHz), but also with a ^{23}Na nucleus (16 MHz).[16] Clearly, sodium mirror leads to the isolated anion $[\mathbf{3}]^{\bullet-}$, while sodium naphthalenide leads to the ion pair $[\mathbf{3}]^{\bullet-}Na^+$; as shown by the coupling constants, spin delocalization on the phosphinine ring is not drastically affected by the presence of the sodium cation. Even by changing the experimental conditions, we could never observe the spectrum of the radical monoanion of the dimeric species $[\mathbf{3}_2]^{\bullet-}$ which is expected to exhibit hyperfine interaction with two equivalent ^{31}P nuclei.

Cyclic Voltammetry. Four reduction-waves are observed at −1.85, −2.10, −2.31, and −2.65 V on the voltammogram of a solution of **1** in THF (2 mM, 20 °C). With a scan rate of 5 V s^{-1}, the waves at −1.85 and −2.10 V were found to be quasi-reversible.

II.2. DFT Calculations. Due to the large size of **1**, calculations were carried out on the model molecule **I** where the phenyl groups were replaced by hydrogen atoms. Two conformations $\mathbf{I_a}$ and $\mathbf{I_b}$ exist, a priori, for this molecule. As mentioned above, X-rays diffraction shows that, in the crystal state, both the neutral molecule **1** and the dianion $[\mathbf{1}]^{2-}$ adopt the **a** conformation; we will therefore concentrate on the $\mathbf{I_a}$ structure[17] (Chart 5).

Chart 5

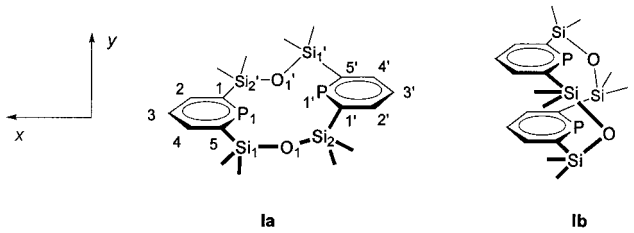

Calculations were first performed on the neutral molecule by assuming C_i and C_{2h} symmetries. The minimum energy was found for the C_{2h} conformer, all the frequencies calculated for this optimized structure were found to be positive. Since the corresponding geometry was found to be appreciably different from that obtained from the crystal structure of **1**, additional optimizations were performed in the C_1 symmetry by using, as starting geometry, the atomic coordinates given by the crystal structure. The resulting geometry was practically the same as that previously calculated in the C_{2h} symmetry. The geometric parameters obtained for the optimized structure of $\mathbf{I_a}$, as well as those obtained from the crystal structure of **1**, are shown in Table 1. For these two geometries the two phosphinine planes are parallel; however, whereas they are almost perpendicular to the P−P direction in the optimized structure, they make an angle of 128° with this direction in the crystal. This change is accompanied by a decrease of 14° in the Si−O−Si bond angle. These differences result in a shortening of the P···P distance which passes from 3.724 Å in $\mathbf{I_a}$ to 3.256 Å in crystalline **1**. As shown by the crystal structure of **1**, these geometrical modifications are likely to be due to the stacking of the benzene groups in the crystal state.

Table 1. Calculated and Experimental Geometries for **1**, $\mathbf{I_a}$ and Their Anions[a]

	neutral		monoanion	dianion	
	$\mathbf{I_a}$ DFT	**1** crystal	$[\mathbf{I_a}]^{\bullet-}$ DFT	$[\mathbf{I_a}]^{2-}$ DFT	$[\mathbf{1}]^{2-}$ crystal
$P_1\cdots P_{1'}$ (Å)	3.724	3.256	2.763	2.368	2.305
$O_1\cdots O_{1'}$ (Å)	6.846	5.706	7.010	7.406	7.335
P_1-C_1 (Å)	1.755	1.744	1.799	1.854	1.855
C_1-C_2 (Å)	1.402	1.405	1.395	1.391	1.384
C_2-C_3 (Å)	1.397	1.400	1.407	1.413	1.411
$C_1-P_1-C_5$ (deg)	103.79	105.87	102.41	100.85	102.8
$C_2-C_3-C_4$ (deg)	123.26	126.1	122.41	121.93	125.0
$C_4-C_2-C_1-P_1$ (deg)	1.6	1.7	3.7	9.2	7.9
$C_1-C_5-C_4-C_3$ (deg)	0.8	2.7	0.9	2.3	0.1
C_5-Si (Å)	1.897	1.891	1.867	1.840	1.842
Si_1-O_1 (Å)	1.663	1.642	1.669	1.686	1.653
Si−O−Si (deg)	158.02	145.49	152.73	140.06	137.8
C_5-Si-O	109.25	106.24	111.96	114.13	111.8
$C_3-C_2-C_1-Si$	−173.82	177.5	−179.86	−179.89	−178.0
$C_3-C_2-C_1-P_1$	0.89	−3.6	−2.72	−7.02	−3.9
$P_1\cdots O_1$ (Å)	3.897	3.443	3.767	3.888	3.799

[a] Numbering of the atoms corresponds to the labeling shown on the ORTEP representation of **1** (Figure 1).

The optimized structure (C_{2h} symmetry) of the radical anion $[\mathbf{I_a}]^-$ is shown in Table 1. As for $\mathbf{I_a}$, assuming C_1 symmetry practically does not affect this geometry. Optimization of the structure of the dianion $[\mathbf{I_a}]^{2-}$ (in C_{2h} symmetry) leads to the parameters which are given in Table 1 together with those obtained from the crystal structure of $[\mathbf{1}]^{2-}[\{Na(2.2.2)\}_2]^{2+}$. The agreement between calculated and experimental values is very satisfactory.

It is clear, from values reported in Table 1, that successive one-electron additions to $\mathbf{I_a}$ provoke drastic geometry modifications. While the two $C_1C_2C_4C_5$ and $C_{1'}C_{2'}C_{4'}C_{5'}$ planes remain parallel, the Si−O−Si angles diminish (from 158.02° to 152.73° and to 140.06°) and a considerable shortening of the P···P distance occurs which passes from 3.724 to 2.763 Å and to 2.368°. Moreover, as shown by the torsion angles $C_4-C_2-C_1-P_1$ and $C_1-C_5-C_4-C_3$ the reductions are accompanied by a deviation from planarity of the phosphinine ring which progressively adopts a boat conformation. These results are in agreement with the crystal structure measurements on the neutral and

(15) Gerson, F.; Merstetter, P.; Pfenninger, S.; Märkl, G. *Magn. Reson. Chem.* **1997**, *35*, 384.

(16) For ion pairs exhibiting large hyperfine isotropic hyperfine couplings with ^{23}Na, see, for example: (a) Holton, D. M.; Edwards, P. P.; Johnson, D. C.; Page, C. J.; McFarlane, W.; Wood B. *J. Am. Chem. Soc.* **1985**, *107*, 6499. (b) Casewit, C. J.; DuBois, M. R. *Inorg. Chem.* **1986**, *25*, 74.

(17) The results of our DFT calculations on the b conformers are given as Supporting Information.

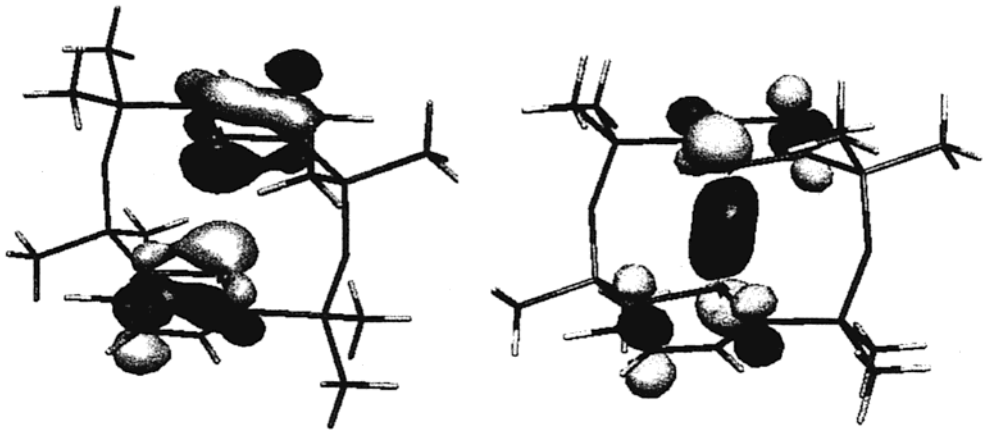

Figure 8. (a) Representation of the HOMO of $\mathbf{I_a}$ calculated by DFT. (b) Representation of the SOMO of $[\mathbf{I_a}]^{\bullet-}$calculated by DFT.

Table 2. Experimental and DFT Calculated EPR Parameters for $[\mathbf{1}]^{\bullet-}$ and $[\mathbf{I_a}]^{\bullet-}$

	g	$^{31}P-A_{iso}$ (MHz) (2 ^{31}P nuclei)	^{31}P-anisotropic coupling (MHz) (2 ^{31}P nuclei)
EPR (liquid spectra) $[\mathbf{1}]^{\bullet-}$	$g_{average}$: 2.0080	(−)10.4	
EPR (frozen solution) $[\mathbf{1}]^{\bullet-}$	$g_i = 2.0097$ $g_j = 2.0088$ $g_k = 2.0039$	(−) 9.9	$\tau_i = (-)47.3$ $\tau_j = (-)77.2$ $\tau_k = (+)124.5$
DFT calculations $[\mathbf{I_a}]^{\bullet-}$		−21.8	$\tau_{\perp 1} = -49.48$ $\tau_{\perp 2} = -64.68$ $\tau_{\parallel} = +114.17^a$

[a] The $\tau_{\parallel}$ eigenvector lies in the $C_3P_1P_{1'}C_{3'}$ plane and makes an angle of 35° with the $P_1P_{1'}$ direction.

dianionic systems: by passing from **1** to $[\mathbf{1}]^{2-}$ the P···P distance drastically decreases and the phosphinyl ring deviates from planarity.

A representation of the HOMO and LUMO for neutral $\mathbf{I_a}$ is shown in Figure 8a. They do not show any participation of the Si−O−Si groups and, due to the large inter-phosphorus distance, the two phosphinine rings appear as being two separate moieties. For $[\mathbf{I_a}]^{\bullet-}$, however, as shown in Figure 8b, a clear overlap of the phosphorus orbitals occurs. The unpaired electron is delocalized in the π system of the two phosphinine rings, and the resulting SOMO is bonding between the two phosphorus atoms. The calculated isotropic and anisotropic phosphorus couplings are given in Table 2, and they reflect large spin densities in the phosphorus p orbitals. The two eigenvectors $\tau_{\parallel}(^{31}P_1)$ and $\tau_{\parallel}(^{31}P_2)$ are aligned along a same direction which lies in the $C_3P_1P_{1'}C_{3'}$ plane and makes an angle of 30° with the $P_1\cdots P_{1'}$ direction. This is consistent with the frozen solution EPR spectrum which was simulated with $\tau_{\parallel}(^{31}P_1)$ and $\tau_{\parallel}(^{31}P_2)$ aligned along a g eigenvector ($g = 2.0039$). Whereas DFT calculations predict an isotropic coupling constant of ∼20 MHz with the protons located para to the phosphorus atoms, no additional proton hyperfine structure could be resolved on the EPR spectra. It is not impossible that intermolecular interaction (stacking between the phenyl groups) increases the pyramidality of the carbon in the para position and, thus, decreases the absolute value of the coupling with this proton.

The structure of $[\mathbf{3}]^{\bullet-}$ was optimized assuming C_s symmetry. The carbon−phosphorus distances (1.83 Å) are found to be close to single C−P bond lengths, and the phosphorus atom lies almost in the $C_1C_2C_4C_5$ mean plane[18] (torsion angle $C_4-C_2-C_1-P = 0.7°$). The calculated isotropic coupling constants with ^{31}P and ^1H (bound to C_3) are equal to 64 and −19 MHz, respectively, in acceptable agreement with the values measured after reduction of **3** with Na.

III. Discussion

In accordance with the voltammogram of **1** which shows that the first reduction wave is reversible and probably corresponds to the formation of the radical monoanion, the EPR spectra obtained after chemical or electrochemical reduction of **1** indicate the formation of a paramagnetic species exhibiting hyperfine interaction from two equivalent ^{31}P nuclei. The magnitude and the relative signs of these isotropic and anisotropic coupling constants as well as the mutual orientation of the ^{31}P hyperfine eigenvectors are in good agreement with the DFT results on $[\mathbf{I_a}]^{\bullet-}$ shown in Table 1. These calculations show that the equivalency of the two isotropic ^{31}P couplings is not dynamic in nature but is due to two equivalent nuclei (set 2 mentioned in the Results). Following the usual method, comparison of the experimental anisotropic and isotropic constants with the atomic parameters leads, for each phosphorus atom, to an approximate spin density of 0.165 in a p orbital and a very small s character. This is in good accordance with the SOMO represented in Figure 8b and which shows a large participation of the phosphorus p_x and p_y atomic orbitals.

Whereas the distance between the two phosphorus atoms is larger than 3 Å in both neutral macrocycles **1** and $\mathbf{I_a}$ (3.256 Å from the crystal structure of **1**, 3.724 Å for the DFT optimized structure of $\mathbf{I_a}$), one-electron reduction of these molecules brings the two phosphorus atoms closer together. The resulting calculated P···P distance (2.763 Å) is clearly less than twice the phosphorus van der Waals radius (3.8 Å) and, as indicated by the experimental and calculated coupling constants corresponds to the formation of a new bond. This bond is considerably longer than the usual P−P bond length (2.1 Å),[19] and it slightly exceeds the one-electron bond length (2.635 Å) recently reported by Bertrand et al.[3] for a compound resulting from the dimerization of a diphosphirenyl radical. Clearly, the formation of this P−P bond in $[\mathbf{1}]^{\bullet-}$ is ensured by the macrocycle which, by maintaining the two phosphorus atoms closer together, allows the extra electron to be accommodated in a SOMO which has a bonding character between them. This electronic structure is quite reminiscent of the intramolecular boron−boron one-electron σ bond which has been very recently described by Hoefelmeyer and Gabbaï[20] and of the structure reported for

(18) Numbering of the atoms is the same as for the phosphinine moiety of $[\mathbf{3}]_2^{2-}[Na(THF)_2]^+_2$ shown in Figure 5.

(19) Cowley, A. H. *Chem. Rev.* **1965**, *65*, 617; Durig, J. R.; Carreira, L. A.; Odom, J. D. *J. Am. Chem. Soc.* **1974**, *96*, 2688.

benzene radical anion dimer.[21] As shown by the crystal structure of the dianion, addition of a second electron in this orbital decreases the interphosphinine bond length (2.305(2) Å) which becomes almost equal to that of a common P−P bond (2.1 Å). The role of the macrocycle for the one-electron bond formation in the radical anion is confirmed by the EPR spectra recorded after reduction of a solution of **3**. In this case the hyperfine structure is caused by the coupling with a single ^{31}P nucleus and proves that no phosphorus−phosphorus bond is formed in absence of interphosphinine connecting Si−O−Si chain. However, any other constraint which forces the two phosphinine rings to adopt the adequate orientation is likely to give rise to the "dimeric" species. This is just what happens during crystallization of the sodium complex of **3**: in this process, when the local concentration is sufficiently high, two phosphinine monoanions share two sodium counterions to form a system composed of two ion pairs. In this system, the $C^{\delta-}Na^{+}P^{\delta-}$ interaction stabilizes a polycyclic structure where the phosphinine ring adopts a boat conformation and where the relative position of the two phosphorus atoms (internuclear distance and orientation of the π orbitals) is suitable for the formation of a P−P bond. The molecular organization of this species is quite different from that observed for the macrocycle dianion $[\mathbf{1}]^{2\bullet-}$; nevertheless, in each case, the interphosphinine bond of the dianion is similar to the common P−P bond length distance (2.286(2) for $[(\mathbf{3})_2]^{2-}$, 2.305(2) for $[\mathbf{1}]^{2-}$).

Concluding Remarks

In this paper we have shown that a new type of phosphorus−phosphorus bond can be formed by reducing a system in which two phosphinine rings are forced to be parallel, with the P···P direction oriented perpendicular to the ring plane. The required geometry can be brought about by incorporating the phosphinines in a macrocycle. In the resulting radical monoanion, the P−P bond, clearly detected from the hyperfine coupling with two equivalent ^{31}P nuclei, is predicted to be equal to 2.7 Å from DFT calculations. This long one-electron bond involves essentially the σ overlap of two phosphorus p orbitals almost perpendicular to the phosphinine plane. As shown by the crystal structure, addition of a second electron decreases the bond length to 2.305 Å. In the absence of constraints due to the macrocycle (e.g., **3**) , the radical monoanion remains isolated in the solution, the paramagnetic species with the slack P−P bond is not observed. During crystallization, however, a new architecture implying C··Na··P interactions is created, the phosphininide monoradical anion dimerizes, and in the resulting diamagnetic dianion an usual P−P bond is formed. The formation of the weak P−P bond observed in $[\mathbf{1}]^{\bullet-}$ illustrates the role played by a rigid molecular environment in a molecular transformation and is somewhat reminiscent of transformations occurring at an enzymatic site. Experiments are in progress to show that the formation of the one-electron P−P bond by applying a reduction potential can be used as a molecular switch.

IV. Experimental Section

IV.1. Compounds. General Considerations. All reactions were routinely performed under an inert atmosphere of argon or nitrogen by using Schlenk and glovebox techniques and dry deoxygenated solvents. Apart from **1** and **3** which can be handled in air, all other compounds are very sensitive and must be handled in the glovebox. Dry THF was obtained by distillation from Na/benzophenone. Deuterated solvents were dried with 4 Å Linde molecular sieves. Nuclear magnetic resonance spectra were recorded on a Bruker AC-200 SY spectrometer operating at 200.13 MHz for ^{1}H, 50.32 MHz for ^{13}C, and 81.01 MHz for ^{31}P. Solvent peaks are used as internal reference relative to Me_4Si for ^{1}H and ^{13}C chemical shifts (ppm); ^{31}P chemical shifts are relative to a 85% H_3PO_4 external reference. Coupling constants are given in hertz. The following abbreviations are used: b, broad; s, singlet; d, doublet; t, triplet; m, multiplet; v, virtual. Diazaphosphinine **2** was prepared according to reported procedures.[11]

Reduction of 1, Synthesis of $[\mathbf{1}]^{2-}[\{Na(2.2.2)\}_2]^{2+}$. Macrocycle **1** (120 mg, 0.16 mmol) was placed under vacuum in a Schlenk tube and taken to a glovebox. The flask was filled with argon and 2 equiv (which corresponds to 1 equiv per phosphinine subunit) of sodium naphthalenide (3.16 mL from a 1×10^{-4} mol/mL solution in THF) was slowly added on the solid. Addition of cryptand (2.2.2) (120 mg, 0.32 mmol) provoked a slow precipitation of $[\mathbf{1}]^{2-}[\{Na(2.2.2)\}_2]^{2+}$. After 3 h at room temperature, the dark-violet solid was recovered by filtration in the glovebox. Yield: 185 mg (75%). Complex $[\mathbf{1}]^{2-}$ can also be isolated as a noncryptated salt of general formula $[\mathbf{1}]^{2-}[\{Na(THF)_2\}_2]^{2+}$ for NMR characterizations. After addition of sodium naphthalenide, the greenish-brown solution obtained was taken out of the box and evaporated to dryness, resulting in the sublimation of the naphthalene. The residue was taken back into the glovebox and dissolved in d_8-THF to record the ^{31}P, ^{1}H, and ^{13}C NMR spectra. This compound is highly sensitive to traces of moisture and oxygen.

^{31}P NMR (C_4D_8O): δ 2.5 (s) (THF solvated species) and 8.8 (s) (cryptated species). ^{1}H NMR (C_4D_8O): δ −0.89 (bs, 12H, $SiMe_2$), 0.00 (bs, 12H, $SiMe_2$), 5.00 (bs, 2H, CH_γ), 7.0−7.3 (m, 20H, Ph); ^{13}C NMR (C_4D_8O): δ 1.5 (s, $SiMe_2$), 3.8 (s, $SiMe_2$), 93.0 (vt, AXX′, ΣJ(C−P) = 34.5, C_α), 100.6 (vt, AXX′, ΣJ(C−P) = 7.7, C_γ), 126−130 (Ph), 150.8 (s, C_q of Ph), 157.7 (vt, ΣJ(C−P) = 4.7, C_β).

Synthesis of 2,6-Bis(trimethylsilyl)-3,5-dimethylphosphinine 3. The following scheme was followed: diazaphosphinine **2** (840 mg, 4 mmol) and trimethylsilylpropyne (2.24 g, 20 mmol) were heated at 110 °C in toluene for 15 h. The excess of alkyne and toluene were then removed under vacuum and phosphinine **3** was purified by column chromatography using hexane as eluant. After evaporation of solvents **3** was recovered as a colorless solid. Yield: 860 mg (80%).

^{31}P NMR ($CDCl_3$): δ 265.0 (s); ^{1}H NMR ($CDCl_3$): δ 0.41 (d, ^{4}J(H−P) = 1.7, $SiMe_3$), 2.57 (d, ^{4}J(H−P) = 1.6, Me), 7.09 (s, H_4); ^{13}C NMR ($CDCl_3$): δ 1.9 (d, ^{3}J(C−P) = 10.6, $SiMe_3$), 26.8 (s, Me), 133.9 (d, ^{3}J(C−P) = 22.8, C_4), 150.4 (d, ^{2}J(C−P) = 11.1, $C_{3,5}$), 164.0 (d, ^{1}J(C−P) = 84.1, $C_{2,6}$).

Reduction of 2,6-Bis(trimethylsilyl)-3,5-dimethylphosphinine 3, Synthesis of $[(\mathbf{3})_2]^{2-}[\{Na(THF)_2\}_2]^{2+}$. Phosphinine **3** (120 mg, 0.45 mmol) was weighed in air, placed under vacuum in a Schlenk tube, and taken to a drybox. The flask was filled with argon, and 1 equiv of sodium naphthalenide (4.46 mL from a 1×10^{-4} mol/mL solution in THF) was slowly added to the solid. Green crystals deposited within 5 min. The mixture was then taken out of the box and evaporated to dryness which resulted in the sublimation of the naphthalene. The low solubility of the compound precluded the recording of the ^{13}C spectrum. $[(\mathbf{3})_2]^{2-}[\{Na(THF)_2\}_2]^{2+}$ was isolated as a highly oxygen- and moisture-sensitive compound. Yield: 156 mg (80%).

^{31}P NMR (C_4D_8O): δ −68.5 (bs); ^{1}H NMR (C_4D_8O): δ 0.11 (bs, 36H, $SiMe_3$), 2.00 (bs, 12H, Me), 4.62 (bs, 2H, H_4).

IV.2. X-ray Diffraction Studies. Crystals of **1** were obtained by a slow diffusion of methanol in a toluene solution of the compound at room temperature. Crystals of $[\mathbf{1}]^{2-}[\{Na(2.2.2)\}_2]^{2+}$ and $[(\mathbf{3})_2]^{2-}[\{Na(THF)_2\}_2]^{2+}$ were isolated from THF solutions of the compounds at room temperature in sealed tubes. The tubes were then broken in the glovebox, and crystals were protected with paratone oil for handling and then submitted to X-ray diffraction analysis. Data were collected on a Nonius Kappa CCD diffractometer using an Mo Kα ($\lambda = 0.71070$ Å) X-ray source and a graphite monochromator. Experimental details are described in Table 3. The crystal structures were solved using SIR 97[22] and Shelxl-97.[23] ORTEP drawings were made using ORTEP III for Windows.[24]

(20) Hoefelmeyer, J. D.; Gabbaï, F. P. *J. Am. Chem. Soc.* **2000**, *122*, 9054.

(21) Hitchcock, P. B.; Lappert, M. F.; Protchenko, A. V. *J. Am. Chem. Soc.* **2001**, *123*, 189.

(22) SIR97, an integrated package computer programs for the solution and refinement of crystal structures using single-crystal data: Altomare, A.; Burla, M. C.; Camalli, M.; Gascarno, G.; Giacovazzo, C.; Guagliardi, A.; Moliterni, A. G. G.; Polidori, G.; Spagna, R.

(23) Sheldrick, G. M. *SHELXL-97*, Programs for Crystal Structure Analysis (Release 97-2); Universität Göttingen: Göttingen, Germany, 1998.

Table 3. Crystallographic Data and Experimental Parameters for the Structure of Compounds **1**, $[\mathbf{1}]^2$ $[\{Na(2.2.2)\}_2]^{2+}$, and $[(\mathbf{3})_2]^{2-}[\{Na(THF)_2\}_2]^{2+}$

	1	$[\mathbf{1}]^{2-}[\{Na(2.2.2)\}_2]^{2+}$	$[(\mathbf{3})_2]^{2-}[\{Na(THF)_2\}_2]^{2+}$
mol formula	$C_{42}H_{46}O_2P_2Si_4$	$C_{78}H_{116}N_4Na_2O_{14}P_2Si_4$	$C_{42}H_{82}Na_2O_4P_2Si_4$
mol wt	757.09	1554.03	871.36
cryst description	colorless cube	purple needle	dark green plate
(habit/size (mm))	0.18 × 0.18 × 0.18	0.16 × 0.10 × 0.10	0.40 × 0.40 × 0.20
cryst syst	orthorhombic	triclinic	monoclinic
space group	Pbca	*P*-1	*C*2/*c*
a (Å)	16.4473(7)	13.097(5)	12.5233(3)
b (Å)	10.9148(3)	13.449(5)	18.5175(6)
c (Å)	22.4703(9)	13.914(5)	22.5328(7)
α (deg)	90.000(2)	78.410(5)	90.00
β (deg)	90.000(2)	65.960(5)	102.864(2)
γ (deg)	90.000(2)	62.950(5)	90.00
V (Å^3)	4033.8(3)	1993.0(13)	5094.2(3)
Z	4	1	4
d (g/cm^3)	1.247	1.295	1.136
F(000)	1600	832	1896
μ (cm^{-1})	0.261	0.190	0.232
T(K)	150.0(1)	150.0(1)	150.0(1)
max Θ (deg)	27.54	23.25	30.01
hkl ranges	−21 16; −14 13;−29 26	−13 14;−14 14;−15 15	−17 17; −26 23; −21 31
no. of rflns measd	20248	9722	17596
no. of indep rflns	4267	5708	7393
no. of rflns used	3649	4479	6312
R_{int}	0.0621	0.0521	0.0379
refinement type	Fsqd	Fsqd	Fsqd
hydrogen atoms	mixed	mixed	mixed
no. of parameters refined	230	473	262
rfln/param ratio	15	9	24
wR2	0.1090	0.1233	0.1416
R1	0.0397	0.0650	0.0513
criterion	$>2\sigma(I)$	$>2\sigma(I)$	$>2\sigma(I)$
GOF	1.015	1.113	1.030
diff peak/hole (e Å^3)	0.394 (0.055)/−0.359(0.055)	0.713 (0.058)/−0.536(0.058)	0.557(0.058)/−0.644(0.058)

IV.3. Cyclic Voltametry. Transient cyclic voltammetry was performed in ca. 12 mL three-electrode airtight cell connected to a Schlenck line. The working electrode consisted of a gold disk of 0.5 mm diameter made from a cross-section of a gold wire (Goodfellow) sealed in glass. The reference electrode was an SCE (Tacussel), separated from the solution by a bridge (3 mL) filled with a 0.3 M solution of *n*-Bu_4NBF_4 in THF identical to the one used in the cell. The counter electrode was a platinum spiral of ca. 1 cm^2 apparent surface located within 5 mm of the working electrode and facing it. An electrochemical digital analyzer DEA-I (Radiometer Copenhagen), which includes a DEA 332 potentiostat with positive feedback for ohmic drop compensation, was used for the experiments.

IV.4. EPR Spectroscopy. EPR experiments were carried out on a Bruker 200D and a Bruker ESP-300 spectrometers (X-band, 100 kHz field modulation) equipped with a variable-temperature attachment. Freshly distilled and degassed solvents were used for the preparation of the samples. Electrochemical generation of the radical anions was performed by in situ electrolysis in the EPR cavity by using platinum electrodes and tetrabutylammonium hexafluorophosphate (0.1 M) as an electrolyte together with a Princeton Applied Research potentiostat. The alkaline metal mirrors used for the chemical reduction of the samples were formed by subliming the metal, under high vacuum (10^{-5} Torr), in a quartz device containing the frozen solution of phosphinine in THF, DME, or CH_2Cl_2; the quartz tube was sealed before reacting the solution on the metal mirror, and then the resulting sample was directly inserted in the EPR cavity. The frozen solution spectra were simulated and optimized using a program[25] based on the Levenberg−Marquardt algorithm: in this program the experimental resonance positions are compared to the values calculated with second-order perturbation theory, the elements of the nondiagonalized **g** and hyperfine tensors are optimized by taking 38000 arbitrary orientations of the magnetic field with respect to the paramagnetic molecule.

IV.5. DFT Calculations. Spin-unrestricted calculations were carried out with the Gaussian 98 package[26] using B3LYP functional.[27] The 6-31G* and the 6-31+G* basis sets were used for neutral and anionic systems, respectively. The optimized geometries were characterized by harmonic frequency analysis (all frequencies real). The molecular orbitals were visualized with the Molekel program[28] by carrying out a single-point restricted-DFT calculation at the optimized geometry.

Acknowledgment. The authors thank the Swiss National Science Foundation, the CNRS, and the Ecole Polytechnique for financial support.

Supporting Information Available: Tables of crystal data, atomic coordinates and equivalent isotropic displacements parameters, bond lengths and angles, anisotropic displacements parameters, hydrogen coordinates, and equivalent isotropic displacement parameters for **1**, $[\mathbf{1}]^{2-}$ $[Na(2.2.2)]_2^+$, $[(\mathbf{3})_2]^{2-}[\{Na(THF)_2\}_2]^{2+}$; ^{31}P hyperfine tensors used for the simulation of the frozen solution spectra, table of geometrical parameters for $\mathbf{I_b}$ (PDF). This material is available free of charge via the Internet at http://pubs.acs.org.

JA010331R

(24) Farrugia, L. J.; ORTEP-3 for Windows, v.1.602. *J. Appl. Crystallogr.* **1997**, *30*, 565.

(25) Soulié, E.; Berclaz, T.; Geoffroy, M. *AIP Conference Proceedings 330, Comput. Chem.* **1996**, 627. Bernardi, F., Rivail, J-L., Eds.

(26) Frisch, M. J.; Trucks, G. W.; Schlegel, H. B.; Scuseria, G. E.; Robb, M. A.; Cheeseman, J. R.; Zakrzewski, V. G.; Montgomery, J. A., Jr.; Stratmann, R. E.; Burant, J. C.; Dapprich, S.; Millam, J. M.; Daniels, A. D.; Kudin, K. N.; Strain, M. C.; Farkas, O.; Tomasi, J.; Barone, V.; Cossi, M.; Cammi, R.; Mennucci, B.; Pomelli, C.; Adamo, C.; Clifford, S.; Ochterski, J.; Petersson, G. A.; Ayala, P. Y.; Cui, Q.; Morokuma, K.; Malick, D. K.; Rabuck, A. D.; Raghavachari, K.; Foresman, J. B.; Cioslowski, J.; Ortiz, J. V.; Stefanov, B. B.; Liu, G.; Liashenko, A.; Piskorz, P.; Komaromi, I.; Gomperts, R.; Martin, R. L.; Fox, D. J.; Keith, T.; Al-Laham, M. A.; Peng, C. Y.; Nanayakkara, A.; Gonzalez, C.; Challacombe, M.; Gill, P. M. W.; Johnson, B. G.; Chen, W.; Wong, M. W.; Andres, J. L.; Head-Gordon, M.; Replogle, E. S.; Pople, J. A. *Gaussian 98*, revision A.7; Gaussian, Inc.: Pittsburgh, PA, 1998.

(27) Becke, A. D. *J. Chem. Phys.* **1993**, *98*, 5648.

(28) Flukiger, P. Development of Molecular Graphics Package MOLEKEL. Ph.D. Thesis, University of Geneva, Switzerland, 1992.